Cek Turnitin - Jurnal - UiO-66 and ZIF-8 Metal-organic Frameworks for Acenaphthene Adsorption

by Cek Turnitin Jurnal

Submission date: 19-May-2023 11:45AM (UTC+0700)
Submission ID: 2096816023
File name: UiO-66_and_ZIF-8_Metal-organic.pdf (442.27K)
Word count: 5716
Character count: 27145

UiO-66 and ZIF-8 Metal-organic Frameworks for Acenaphthene Adsorption

Chapter · January 2021

DOI: 10.1007/978-981-16-4513-6_21

4 authors:

Zakariyya Uba Zango
Universiti Teknologi PETRONAS
59 PUBLICATIONS **676** CITATIONS
SEE PROFILE

Anita Ramli
Universiti Teknologi PETRONAS
163 PUBLICATIONS **2,877** CITATIONS
SEE PROFILE

Khairulazhar Jumbri
Universiti Putra Malaysia
67 PUBLICATIONS **694** CITATIONS
SEE PROFILE

Muslim Bin Darbi Abdurrahman
Universitas Islam Riau
65 PUBLICATIONS **248** CITATIONS
SEE PROFILE

UiO-66 and ZIF-8 Metal-organic Frameworks for Acenaphthene Adsorption

Zakariyya Uba Zango, Anita Ramli, Khairulazhar Jumbri, and Muslim Abdurrahman

Abstract Comparative adsorption of acenaphthene onto UiO-66 and ZIF-8 metal-organic frameworks (MOFs) were investigated. Response surface methodology (RSM) was employed for the process optimizations according to the central composite design (CCD) with 5 inputs variables. The adsorption efficiency achieved were 99.7 and 60.7% for the UiO-66 and ZIF-8, respectively according to the RSM optimization conditions. The model was significantly described according to statistical analysis of variance (ANOVA). The adsorption process was well fitted by pseudo-second order kinetic model with R^2 values of 0.9947 and 0.97780 for the UiO-66 and ZIF-8, respectively.

Keywords Acenaphthene · Adsorption · Metal-organic frameworks · Response surface methodology

Z. U. Zango · A. Ramli (✉) · K. Jumbri
Department of Fundamental and Applied Sciences, Universiti Teknologi PETRONAS, 3210 Seri Iskandar, Perak, Malaysia
e-mail: anita_ramli@utp.edu.my

K. Jumbri
e-mail: khairulazharjumbri@utp.edu.my

Z. U. Zango
Department of Chemistry, Al-Qalam University Katsina, Katsina 2137, Nigeria

A. Ramli
HiCOE Centre for Biofuel and Biochemical Research (CBBR), Universiti Teknologi PETRONAS, 3210 Seri Iskandar, Perak, Malaysia

K. Jumbri
Centre of Research in Ionic Liquids (CORIL), Universiti Teknologi PETRONAS, 3210 Seri Iskandar, Perak, Malaysia

M. Abdurrahman
Department of Petroleum Engineering, Universitas Islam Riau, Jalan Kaharuddin Nasution No. 113, Pekanbaru 28284, Indonesia
e-mail: muslim@eng.uir.ac.id

S. A. Abdul Karim et al. (eds.), *Proceedings of the 6th International Conference on Fundamental and Applied Sciences*, Springer Proceedings in Complexity,
https://doi.org/10.1007/978-981-16-4513-6_21

1 Introduction

Pollution caused by the presence of organic contaminants in environmental waters has been a disturbing phenomenon affecting the peaceful existence of living organisms. Acenaphthene, a member of Polycyclic aromatic carbons (PAHs) heavily found in crude oil and coal [1, 2]. It consisted of naphthalene connected by the ethylene at position 1 and 8 (Fig. 1). It also occurs in small quantity as a result of biomass decay [3]. It has found variety of applications in industrial processing as a precursor and intermediate material for the production of products such as dyes production, plastics, insecticides, fungicides and other manufacturing processes [4, 5]. It is an important component in coal tar for road and highway constructions and as preservative in wood industries [6]. It is among the most prominent organic pollutant ubiquitously found in environmental waters [7]. It is resulted from oil spillage, effluents discharged from petroleum and petrochemical industries, coal conversion process, urban air due to automobile exhaust and cigarette smoke, as well as municipal wastewater due to the soil surface and street asphalt runoff [8, 9]. It is relatively insoluble in water (0.4 mg/100 mL), thus easily transported into the water bodies. Findings have shown the presence of acenaphthene in various ground and surface waters. It is recalcitrant to atmospheric degradation, thus undergoes bioaccumulation in the soil and sediments and subsequently consumed by the plants and aquatic organisms [10]. It was known to cause significant impact to both plants and animals due to its toxic and hazardous effects such as eye and skin irritations, lungs cancer and other respiratory complications [11, 12]. It was listed among the priority PAHs organic pollutant according to USEPA. Thus, essentially required to be eliminated from environmental waters.

Adsorption process have been recognized as an alternative wastewater remediation technology. It is a low-cost and environmental-friendly technique for variety of pollutants removal from the water. The availability of various natural and synthetic adsorbents materials for both organic and inorganic pollutants removal has been capitalized as the way forward compared to other water treatment technologies such as coagulation, reverse osmosis and enzymatic degradation processes [13, 14]. Thus, various adsorbents from natural and sources such as biomass [15], clays, soil and sand particles [16], etc., have been well reported for the acenaphthene adsorption from environmental waters. Despite showing lots of promise in water treatment, most of these adsorbents are not suitable for PAHs removal from water due to the low specific

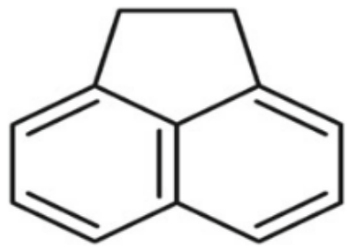

Fig. 1 Chemical structure of acenaphthene

surface area and pore volumes of the adsorbents [17]. The use of synthetic materials such as activated carbons [18], biochar [19], carbon nanotubes, graphene [20], and silica have also been reported. However, AC is not suitable for organic pollutant removal at low concentrations.

Advancement in materials sciences have paved the way for the invention of new classes of materials with versatile applications. Metal-organic frameworks (MOFs) are among the most advanced materials that attracted the attention of researchers from scientific and engineering fields. They are comprised of coordination sphere made from interaction of metal-ion with organic moieties, forming extensive crystalline frameworks [21, 22]. They acquired unique properties such as exceptionally high porosities, mechanical and thermal strength [23, 24]. Thus, they have found tremendous applications in various fields such as carbon dioxide capture, energy storage, sensors, drug delivery, catalysis and wastewater remediations [25, 26]. They offered promising applications as super adsorbents for both organic and inorganic pollutants removal from water [27–29], due to their ultrahigh porosities and good stabilities.

This work is thus aimed at adsorption of acenaphthene from aqueous medium using UiO-66 and ZIF-8 MOFs. They were chosen due to their high BET surface area and pore volumes as well as their stabilities in both aqueous and organic phases. Response surface methodology (RSM) was used for the experimental design using central composite design (CCD). The kinetics of the adsorption process was evaluated, and the reusability of the MOFs was studied.

2 Materials and Methods

The materials purchased in this work were analytically graded and thus were used as received. Acenaphthene standard (99% purity), ZIF-8 (99% purity) zirconium tetrachloride (99.99% purity), terephthalic acid (97% purity) obtained from Sigma Aldrich (USA), and supplied by Avantis Laboratory, Malaysia.

2.1 Synthesis and Characterizations of the MOFs

UiO-66 was synthesized and characterized according to the procedure reported in our previous work [30]. While ZIF-8 was commercially purchased.

2.2 Preparation of the Stock Solution

The acenaphthene stock solution was prepared in acetone by using 10 mg of the standard in 100 ml volumetric flask to make a solution of 100 mg/L. Working solution was prepared from the stock solution in double deionized water using serial dilutions.

2.3 Synthesis of the MOFs

Batch adsorption experiment was designed by the RSM software (Design Expert 11) using full factorial CCD comprises of 5 input variables: contact time (min), dosage (mg), concentration (mg/L), pH and temperature (°C) with 5 center points. The adsorption was conducted using 30 mL of the acenaphthene solution in an incubator shaker (Incubator ES 20/60, bioSan) at 200 rpm. The sample was analyzed using UV-visible spectrophotometer (GENESYS 30) analysis at 220 nm. The responses were determined as the percentage adsorption efficiency achieved by the UiO-66 and ZIF-8 MOFs accordingly to the formula:

$$\%R = \frac{C_0 - C_e}{C_0} \times 100 \tag{1}$$

And the amount of the acenaphthene adsorbed onto the MOFs at certain time (qt) and equilibrium (qe) were determine from the formula:

$$q_t = \frac{(C_0 - C_t)V}{w} \tag{2}$$

$$q_e = \frac{(C_0 - C_e)V}{w} \tag{3}$$

where C_0, C_t and C_e are the initial, time and equilibrium concentrations (mg/L), respectively, w is the weight of adsorbent (g), and V is the volume of the solution (L).

3 Results and Discussion

3.1 RSM Optimizations for Acenaphthene Adsorption onto UiO-66 and ZIF-8

The synthesis of UiO-66 was achieved using solvothermal technique described in our previous studies [30], while ZIF-8 was commercially purchased. The BET surface

area of the MOFs were 1421 m^2/g and 1299 m^2/g, while the pore volumes were 0.91 and 0.60 m^3/g for the UiO-66 and ZIF-8, respectively.

The adsorption studies for the removal acenaphthene were thus conducted using both UiO-66 and ZIF-8. The experimental conditions were determined by the CCD consisting of 5 parameters input variables with 47 number of experimental runs as described in Table 1. The adsorption efficiency of the two MOFs were determined according to each set of the experimental conditions given. The adsorption efficiency of UiO-66 was found to be much higher than that of ZIF-8, which was attributed the higher surface area and pore volume of the MOF [31, 32]. Thus, the highest removal efficiency achieved was 99.7% and 60.7% according to the described multi-variate conditions given in Fig. 2a,b for both UiO-66 and ZIF-8, respectively.

The corresponding 2-dimension (2D) and 3-dimension (3D) graphs for the RSM optimizations of the adsorption process. According to the Fig. 2, the adsorption efficiency was shown to increase with increase in the dosage of the MOFs due to the increase in the available number of adsorption sites on the surface of the MOFs. UiO-66 has shown to efficiently adsorbed larger organic molecules such as dyes and pharmaceuticals from aqueous solutions, attributed to its potential breathing capacity [33], high porosity [34], hydrophobicity and extensive stabilities in both organic and aqueous medium [35]. Similarly, the adsorption efficiency was increase with the increasing the contact time for the adsorption due to the increase in the interaction of the acenaphthene with the surface of the MOFs.

The model fittings were described by the analysis of variance (ANOVA) as presented in Table 2 according to the Fischer test (F-test) and p-values (probability > F) with 95% confidence level for the input variables. The overall model p-values were significant (< 0.0500), with F-value of 33.44 and 126.34 for the UiO-66 and ZIF-8, respectively. The significant terms for the adsorption and parameters combination were A, B, C, D, AD, A^2 and A, B, C, D, AB, BD, A^2 for the UiO-66 and ZIF-8 respectively. The significance of the model was also described by the reasonable agreements between the adjusted R^2 (0.9338 and 0.9820 for UiO-66 and ZIF-8, respectively) and predicted R^2 (0.8733 and 0.9638 for UiO-66 and ZIF-8, respectively) values with less than 20% differences. The lack of fit test for the replicated design points of the residual errors against the pure errors for the model were 0.1915 and 0.5840. The adequate precision of the model was 17.3082 and 32.6708 for the UiO-66 and ZIF-8, respectively, implying that the model can be used to navigate the design space for the adsorption studies. The scatter plots (Fig. 3) have shown significance of the model in terms of good agreement between the experimental and predicted adsorption efficiencies. Thus, RSM model was significant for the design optimizations of acenaphthene adsorption onto UiO-66 and ZIF-8.

3.2 Contact Time and Kinetics Study

The uptake of acenaphthene by the UiO-66 and ZIF-8 MOFs were studied. Adsorption experiment was studied using the optimized RSM data. Figure 4 highlighted the

Table 1 RSM optimizations for acenaphthene adsorption onto UiO-66 and ZIF-8 MOFs

Name	Units	Low	High	− Alpha	+ Alpha
A: Time	min	5	25	0	35
B: Dosage	mg	3	5	2	6
C: Concentration	mg/L	1	3	0	4
D: pH		2	6	0	8
E: Temperature	°C	25	35	20	40

Std	Run	Factor 1	Factor 2	Factor 3	Factor 4	Factor 5	Response 1	Response 2
		Time	Dosage	Concentration	pH	Temperature	UiO-66 (%R)	ZIF-8 (%R)
		min	mg	mg/L		°C		
1	1	5	3	1	2	25	67.3	30.2
3	2	5	5	1	2	25	77.1	33.5
22	3	25	3	3	2	35	84.2	50.2
24	4	25	5	3	2	35	97.5	53.6
14	5	25	3	3	6	25	96.1	51.2
16	6	25	5	3	6	25	98.4	55.2
36	7	15	6	2	4	30	87.4	45.7
45	8	15	4	2	4	30	85.2	44.3
35	9	15	2	2	4	30	72.2	42.1
5	10	5	3	3	2	25	58.5	29.6
17	11	5	3	1	2	35	63.2	31.5
20	12	25	5	1	2	35	98.5	57.4
42	13	15	4	2	4	40	79.3	44.4
7	14	5	5	3	2	25	58.6	33.8
46	15	15	4	2	4	30	79.1	43.6
31	16	5	5	3	6	35	56.3	32.4
33	17	5	4	2	4	30	54.2	32.1
26	18	25	3	1	6	35	95.5	56.3
28	19	25	5	1	6	35	97.1	57.2
32	20	25	5	3	6	35	92.4	55.4
43	21	15	4	2	4	30	77.3	43.7
39	22	15	4	2	10	30	76.2	44.2
18	23	25	3	1	2	35	94.3	56.3
25	24	5	3	1	6	35	55.7	33.5
34	25	35	4	2	4	30	99.7	60.7
2	26	25	3	1	2	25	94.1	56.4
41	27	15	4	2	4	20	76.5	44.5

(continued)

Table 1 (continued)

Std	Run	Factor 1	Factor 2	Factor 3	Factor 4	Factor 5	Response 1	Response 2
		Time	Dosage	Concentration	pH	Temperature	UiO-66 (%R)	ZIF-8 (%R)
		min	mg	mg/L		°C		
10	28	25	3	1	6	25	98.5	56.7
27	29	5	5	1	6	35	57.2	34.8
4	30	25	5	1	2	25	99.1	57.5
8	31	25	5	3	2	25	97.8	55.4
11	32	5	5	1	6	25	59.5	35.1
29	33	5	3	3	6	35	56.4	32.5
15	34	5	5	3	6	25	58.3	33.3
47	35	15	4	2	4	30	77.7	44.2
30	36	25	3	3	6	35	92.6	54.6
21	37	5	3	3	2	35	56.4	32.3
23	38	5	5	3	2	35	58.4	33.6
38	39	15	4	4	4	30	75.5	43.6
44	40	15	4	2	4	30	77.3	45.2
6	41	25	3	3	2	25	91.5	53.7
12	42	25	5	1	6	25	98.5	55.2
9	43	5	3	1	6	25	55.4	33.5
40	44	15	4	2	8	30	77.3	46.3
19	45	5	5	1	2	35	56.4	35.2
13	46	5	3	3	6	25	55.4	33.4
37	47	15	4	5	4	30	75.2	43.2

effect of contact time for the adsorption process. Sudden adsorption of the acenaphthene was observed at the onset of the experiment, attributed to the higher BET surface area of the MOFs [36]. The equilibrium of the adsorption was attained within 30 min with the MOFs achieving equilibrium adsorption capacities of 23.814 mg/g and 14.627 mg/g for UiO-66 and ZIF-8, respectively. The adsorption efficiency achieved at equilibrium was 99.23% and 60.95% for UiO-66 and ZIF-8, respectively, confirming the superior adsorption capacity of UiO-66 and its higher porosities as previously reported in our studies [37].

To understand the mechanism and the rate controlling step for the process, the adsorption data for the UiO-66 and ZIF-8 effect of contact time was kinetics models was treated by the kinetics models of pseudo-first order (Eq. 4), pseudo-second order (Eq. 5), intra-particle diffusion (Eq. 6) and Elovich (Eq. 7) models linearly expressed as.

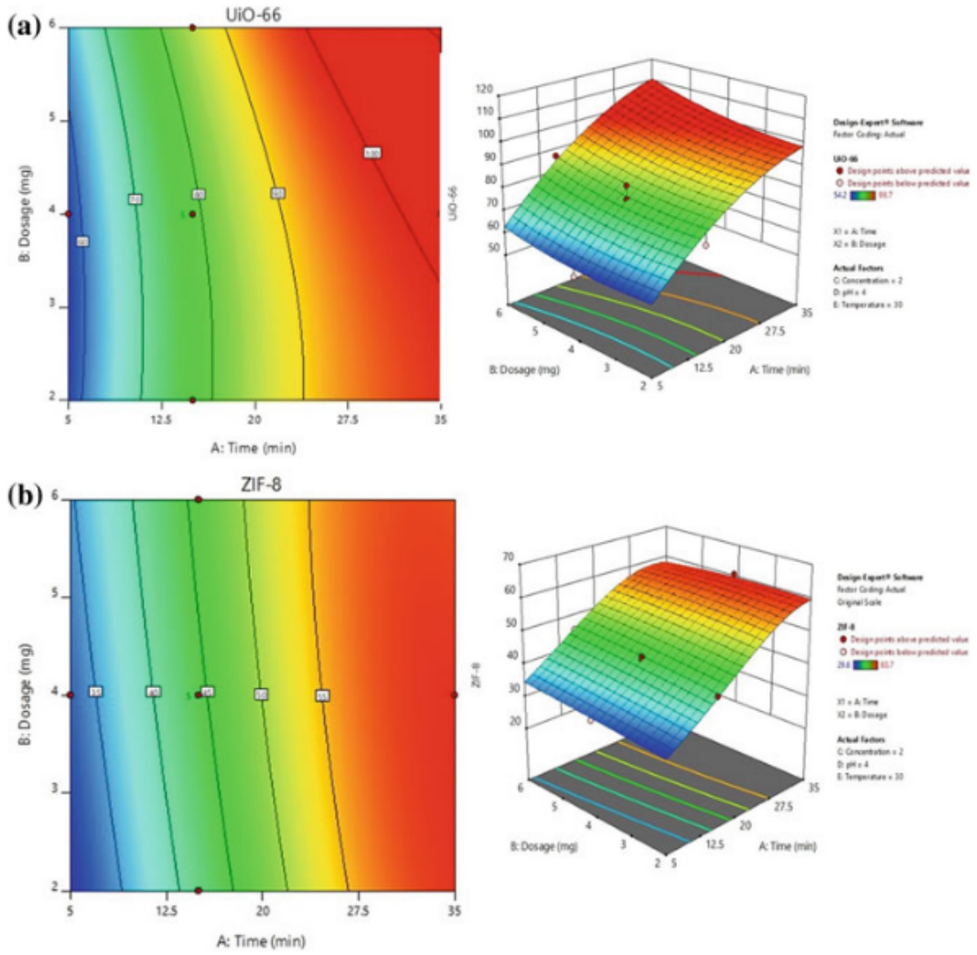

Fig. 2 2D and 3D RSM plots for the adsorption of acenaphthene onto **a** UiO-66 and **b** ZIF-8 MOFs under the condition: contact time of 35 min; dosage of 4 mg; concentrations of 2 mg/L, pH of 4 and temperature of 30 °C

$$\ln(q_e - q_t) = \ln q_e - k_1 t \tag{4}$$

$$\frac{t}{q_t} = \frac{1}{k_2 q_e^2} + \frac{t}{q_e} \tag{5}$$

$$q_t = K_P t^{\frac{1}{2}} + C \tag{6}$$

$$q_t = \frac{1}{\beta} In() + \frac{1}{\beta} Int \tag{7}$$

where q_e (mg/g) and q_t (mg/g) represent the amount of the acenaphthene adsorbed by the MOFs at equilibrium and t (mins). k_1 (1/min) k_2 (q/mg/min) represented the

Table 2 ANOVA for the adsorption of acenaphthene onto UiO-66 and ZIF-8 MOFs

	UiO-66						ZIF-8					
Source	SS	df	MS	F-value	p-value		SS	df	MS	F-value	p-value	
Model	0.0004	20	0.0000	33.44	< 0.0001	Significant	0.0014	20	0.0001	126.34	< 0.0001	Significant
A-Time	0.0004	1	0.0004	636.44	< 0.0001		0.0013	1	0.0013	2455.38	< 0.0001	
B-Dosage	3.434E−06	1	3.434E−06	5.77	0.0238		0.0000	1	0.0000	22.62	< 0.0001	
C-Concentration	3.811E−06	1	3.811E−06	6.40	0.0178		5.770E−06	1	5.770E−06	10.76	0.0029	
D-pH	2.554E−06	1	2.554E−06	4.29	0.0484		3.105E−06	1	3.105E−06	5.79	0.0235	
E-Temperature	1.980E−06	1	1.980E−06	3.33	0.0797		2.672E−07	1	2.672E−07	0.4985	0.4864	
AB	8.016E−09	1	8.016E−09	0.0135	0.9085		3.309E−06	1	3.309E−06	6.17	0.0197	
AC	8.144E−07	1	8.144E−07	1.37	0.2528		1.668E−07	1	1.668E−07	0.3112	0.5817	
AD	4.568E−06	1	4.568E−06	7.67	0.0102		2.068E−06	1	2.068E−06	3.86	0.0603	
AE	7.053E−07	1	7.053E−07	1.18	0.2865		4.333E−07	1	4.333E−07	0.8083	0.3769	
BC	4.427E−08	1	4.427E−08	0.0743	0.7873		2.146E−08	1	2.146E−08	0.0400	0.8430	
BD	2.858E−08	1	2.858E−08	0.0480	0.8283		3.603E−06	1	3.603E−06	6.72	0.0154	
BE	5.467E−07	1	5.467E−07	0.9181	0.3468		2.582E−07	1	2.582E−07	0.4816	0.4938	
CD	1.962E−06	1	1.962E−06	3.30	0.0810		9.847E−08	1	9.847E−08	0.1837	0.6718	
CE	4.490E−07	1	4.490E−07	0.7540	0.3932		2.190E−07	1	2.190E−07	0.4085	0.5283	
DE	7.972E−07	1	7.972E−07	1.34	0.2578		4.070E−07	1	4.070E−07	0.7592	0.3915	
A^2	0.0000	1	0.0000	33.65	< 0.0001		0.0000	1	0.0000	86.03	< 0.0001	
B^2	2.631E−08	1	2.631E−08	0.0442	0.8352		8.056E−08	1	8.056E−08	0.1503	0.7014	
C^2	1.937E−07	1	1.937E−07	0.3253	0.5734		4.969E−07	1	4.969E−07	0.9270	0.3445	
D^2	2.434E−07	1	2.434E−07	0.4088	0.5282		3.000E−07	1	3.000E−07	0.5595	0.4612	
E^2	9.380E−09	1	9.380E−09	0.0158	0.9011		1.998E−08	1	1.998E−08	0.0373	0.8484	

(continued)

Table 2 (continued)

	UiO-66						ZIF-8					
Source	SS	df	MS	F-value	p-value		SS	df	MS	F-value	p-value	
Residual	0.0000	26	5.955E−07				0.0000	26	5.361E−07			
Lack of fit	0.0000	22	6.564E−07	2.52	0.1915	Not significant	0.0000	22	6.146E−07	5.90	0.0484	Not significant
Pure error	1.043E−06	4	2.607E−07				4.170E−07	4	1.043E−07			
Cor total	0.0004	46					0.0014	46				

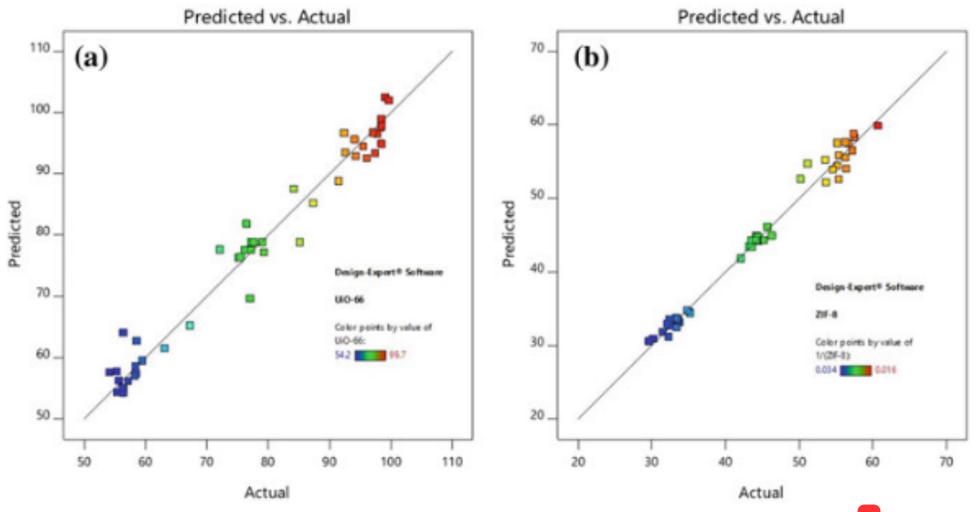

Fig. 3 Scatter plots for the RSM adsorption of acenaphthene onto UiO-66 and ZIF-8 MOFs

Fig. 4 Effect of contact time for the adsorption of acenaphthene onto UiO-66 and ZIF-8 MOFs

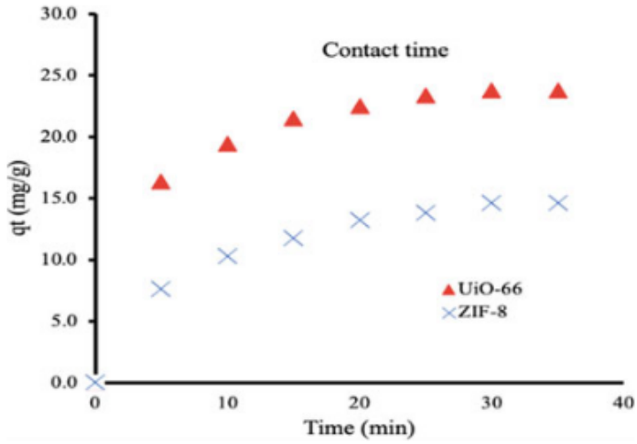

pseudo-first order and pseudo-second order rate constants, respectively. Kp represented the intraparticle rate constant and C is constant. The α (mg/gmin) and β (g/mg) were the initial desorption rate and desorption constant for the Elovich model, respectively.

Figure 5 depicted the plots of the kinetic models studied. The adsorption data was found to be precisely suited by the pseudo-second order model in comparison to other models evaluated. It is R^2 value was 0.9947 and 0.97780 for the UiO-66 and ZIF-8, respectively. Also, its calculated adsorption capacities were 24.80 and 15.87 mg/g for the UiO-66 and ZIF-8, respectively, very closer to the obtained experimental values of 23.814 and 14.627 mg/g for UiO-66 and ZIF-8, respectively, indicating the chemisorption is the rate limiting step of the process and the availability of the adsorption sites on the surface of the MOFs. Other reports have also described

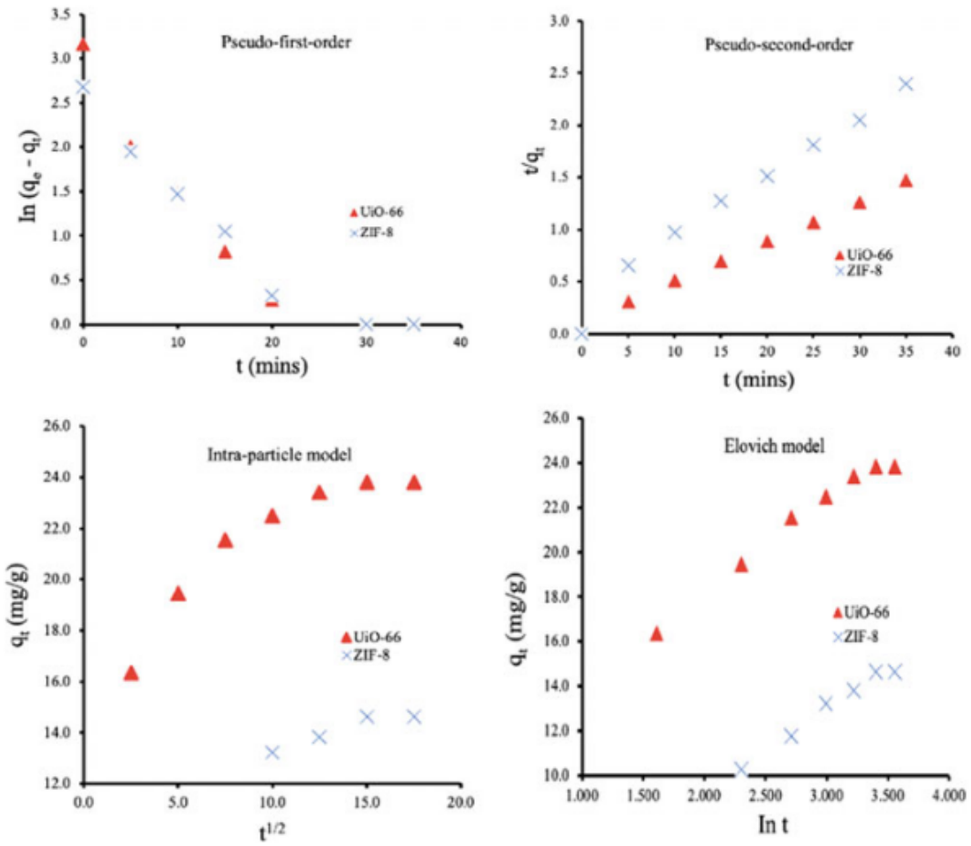

Fig. 5 Adsorption kinetics plots for acenaphthene adsorption onto UiO-66 and ZIF-8 MOFs

the adsorption of organic pollutants onto UiO-66 [38, 39] and ZIF-8 [40, 41] as pseudo-second order process.

4 Conclusion

RSM was used for the experimental design of acenaphthene adsorption onto UiO-66 and ZIF-8 MOFs. Five factor parameters were employed, and best performance of the MOFs was achieved for UiO-66 with adsorption efficiency of 99.7 due to its higher porosity in comparison to ZIF-8 which recorded adsorption efficiency of 60.7%, according to the experimental condition with contact time of contact time of 35 min, dosage of 4 mg, concentrations of 2 mg/L, pH of 4 and temperature of 30 °C. The overall model p-values were significant (< 0.0500) for both UiO-66 and ZIF-8 MOFs. The lack of fit test for the model was insignificant, which was desirable for both MOFs and the adequate precision was 17.3082 and 32.6708 for the UiO-66 and ZIF-8, respectively. Good agreement between the RSM and experimental findings.

Acknowledgements We would like to acknowledge UTP-UIR grant (015MEO-166) received from Universitas Islam Riau Indonesia and FRGS grant (FRGS/1/2020/STG04/UTP/02/3) received from Ministry of Higher Education Malaysia.

References

1. Guieysse, B., Bernhoft, I., Andersson, B.E., Henrysson, T., Olsson, S., Mattiasson, B.: Degradation of acenaphthene, phenanthrene and pyrene in a packed-bed biofilm reactor. Appl. Microbiol. Biotechnol. **54**(6), 826–831 (2000). https://doi.org/10.1007/s002530000442
2. Zango, Z.U., Jumbri, K., Sambudi, N.S., Abu Bakar, N.H.H., Abdullah, N.A.F., Basheer, C., Saad, B.: Removal of anthracene in water by MIL-88(Fe), NH_2-MIL-88(Fe), and mixed-MIL-88(Fe) metal-organic frameworks. RCS Adv. **9**, 41490–41501, (2019). https://doi.org/10.1039/c9ra08660arsc.li/rsc-advances
3. Jiang, L., Zhang, B., Wang, Y., Sun, J., Ma, X., Wang, G., Fu, S., Lin, C., Li, Y.: Three new acenaphthene derivatives from rhizomes of musa basjoo and their cytotoxic activity. Nat. Prod. Res. pp. 1–6 (2019). https://doi.org/10.1080/14786419.2019.1647422
4. Hirano, Y., Iba, Y., Kuroda, N., Kubota, Y., Inagaki, S.: Catalytic carbonization of acenaphthene for the preparation of ordered mesoporous carbon CMK-1 toward application as electrochemical double-layer capacitor electrode with ionic liquid electrolyte. Chem. Lett. **48**(6), 521–524 (2019). https://doi.org/10.1246/cl.190090
5. Bukharkina, T.V., Grechishkina, O.S., Digurov, N.G., Kon'kov, I.I.: Catalytic oxidation of acenaphthene and its derivatives in acetic acid. Org. Process Res. Dev. **6**(4), 394–400 (2002). https://doi.org/10.1021/op0100448
6. Ye, Y.F., Ma, F.Y., Wu, M., Wei, X.Y., Liu, J.M.: Increase of acenaphthene content in creosote oil by hydrodynamic cavitation. Chem. Eng. Process. Process Intensif. **104**, 66–74 (2016). https://doi.org/10.1016/j.cep.2016.03.001
7. Radwan, A.M.Y., Magram, S.F., Ahmed, Z.: Adsorption of acenaphthene using date seed activated carbon. J. Environ. Sci. Technol. **11**(1), 10–15 (2018). https://doi.org/10.3923/jest.2018.10.15
8. Alade, A.O., Amuda, O.S., Ibrahim, A.O.: Isothermal studies of adsorption of acenaphthene from aqueous solution onto activated carbon produced from rice (Oryza sativa) husk. Elixir Chem. Eng. **46**, 87–95 (2012). https://doi.org/10.1080/19443994.2012.677514
9. Rani, C.N., Karthikeyan, S.: Feasibility study of acenaphthene degradation in a novel slurry UV photocatalytic membrane reactor: Effect of operating parameters and optimization using response surface modeling. Chem. Eng. Process.-Process Intensif. pp. 108051 (2020). https://doi.org/10.1016/j.cep.2020.108051
10. Safitri, R., Handayani, S., Surono, W., Astika, H., Damayanti, R., Kusmaya, F.D., Rukiah, Balia, R.L.: Biodegradation of phenol, anthracene and acenaphthene singly and consortium culture of indigenous microorganism isolates from underground coal gasification area. In: IOP Conference Series Earth Environment Science **306**(1) (2019). https://doi.org/10.1088/1755-1315/306/1/012026
11. Gracht Van Der, H.: Potential of lost fishing gears for adsorption of PAHs.Centro Interdisplinar de Investigarcao Marinho e Ambiental (2020)
12. Patrick, U.A., Chiwuike, A.-O.: A column experiment showing adsorption dynamics and kinetics of selected PAH using plantain and cassava peels. Int. J. Adv. Sci. Technol. **111**, 129–146 (2018). https://doi.org/10.14257/ijast.2018.111.12
13. Smol, M., Włodarczyk-Makuła, M., Włóka, D.: Adsorption of polycyclic aromatic hydrocarbons (PAHs) from aqueous solutions on different sorbents. Civ. Environ. Eng. Reports. **13**(2), 87–96 (2014). https://doi.org/10.2478/ceer-2014-0017

14. Huang, Y., Fulton, A.N., Keller, A.A.: Simultaneous removal of PAHs and metal contaminants from water using magnetic nanoparticle adsorbents. Sci. Total Environ. **571**, 1029–1036 (2016). https://doi.org/10.1016/j.scitotenv.2016.07.093
15. Lu, L., Lin, Y., Chai, Q., He, S., Yang, C.: Removal of acenaphthene by biochar and raw biomass with coexisting heavy metal and phenanthrene. Colloids Surfaces A Physicochem. Eng. Asp. **558**, 103–109 (2018). https://doi.org/10.1016/j.colsurfa.2018.08.057
16. Mortazavi, M., Baghdadi, M., Seyed Javadi, N.H., Torabian, A.: The black beads produced by simultaneous thermal reducing and chemical bonding of graphene oxide on the surface of amino-functionalized sand particles: application for PAHs removal from contaminated waters. J. Water Process Eng. **31** (2019). https://doi.org/10.1016/j.jwpe.2019.100798
17. Zango, Z.U., Sambudi, N.S., Jumbri, K., Ramli, A., Hana, N., Abu, H., Saad, B., Nur, M., Rozaini, H., Isiyaka, H.A., Osman, A.M., Sulieman, A.: An overview and evaluation of highly porous adsorbent materials for polycyclic aromatic hydrocarbons and phenols removal from wastewater, pp. 1–40 (2020)
18. Alade, A.O., Amuda, O.S., Afolabi, A.O., Adelowo, F.E.: Adosrption of acenaphthene unto ativated carbon produced from agricultural wastes. J. Envionmental Sci. Technol. **5**(4), 192–209 (2012)
19. Lu, L., Li, A., Ji, X., Yang, C., He, S.: Removal of acenaphthene from water by Triton X-100-facilitated biochar-immobilized pseudomonas aeruginosa. RSC Adv. **8**, 23426–23432 (2018). https://doi.org/10.1039/C8RA03529F
20. Han, B., Li, Y., Qian, B., He, Y., Peng, L., Yu, H.: Adsorption and determination of polycyclic aromatic hydrocarbons in water through the aggregation of graphene oxide. Open Chem. **16**(1), 716–725 (2018). https://doi.org/10.1515/chem-2018-0078
21. Bueken, B., Vermoortele, F., Cliffe, M.J., Wharmby, M.T., Foucher, D., Wieme, J., Vanduyfhuys, L., Martineau, C., Stock, N., Taulelle, F., Van Speybroeck, V., Goodwin, A.L., De Vos, D.: A breathing zirconium metal-organic framework with reversible loss of crystallinity by correlated nanodomain formation. Chem.-A Eur. J. **22**(10), 3264–3267 (2016). https://doi.org/10.1002/chem.201600330
22. Connolly, B.M., Mehta, J.P., Moghadam, P.Z., Wheatley, A.E.H., Fairen-Jimenez, D.: From synthesis to applications: metal-organic frameworks for an environmentally sustainable future. Curr. Opin. Green Sustain. Chem. **12**, 47–56 (2018). https://doi.org/10.1016/j.cogsc.2018.06.012
23. Adesina Adegoke, K., Samuel Agboola, O., Ogunmodede, J., Oluyomi Araoye, A., Solomon Bello, O.: Metal-organic frameworks as adsorbents for sequestering organic pollutants from wastewater. Mater. Chem. Phys. **253**, p. 123246 (2020). https://doi.org/10.1016/j.matchemphys.2020.123246
24. Gomar, M., Yeganegi, S.: Adsorption of 5-fluorouracil, hydroxyurea and mercaptopurine drugs on zeolitic imidazolate frameworks (ZIF-7, ZIF-8 and ZIF-9). Microporous Mesoporous Mater. **252**, 167–172 (2017). https://doi.org/10.1016/j.micromeso.2017.06.010
25. Jin, Z., Yang, H.: Exploration of Zr-metal-organic framework as efficient photocatalyst for hydrogen production. Nanoscale Res. Lett. **12** (2017). https://doi.org/10.1186/s11671-017-2311-6
26. Zango, Z.U., Jumbri, K., Sambudi, N.S., Ramli, A., Bakar, N.H.H.A., Saad, B., Rozaini, M.N.H., Isiyaka, H.A., Jagaba, A.H., Aldaghri, O., Sulieman, A.: A critical review on metal-organic frameworks and their composites as advanced materials for adsorption and photocatalytic degradation of emerging organic pollutants from wastewater. Polymers (Basel). **12**, 1–42 (2020). https://doi.org/10.3390/polym12112648
27. Zango, Z.U., Ramli, A., Jumbri, K., Sambudi, N.S., Isiyaka, H.A., Abu Bakar, N.H.H., Saad, B.: Response surface methodology optimization and kinetics study for anthracene adsorption onto MIL-88(Fe) and NH_2-MIL-88(Fe) metal- organic frameworks. In: Series IOP Conference Science Materials **88**, pp. 0–12 (2021). https://doi.org/10.1088/1757-899X/1092/1/012035
28. Petit, C.: Present and future of MOF research in the field of adsorption and molecular separation. Curr. Opin. Chem. Eng. **20**, 132–142 (2018). https://doi.org/10.1016/j.coche.2018.04.004

29. Shahmirzaee, M., Hemmati-Sarapardeh, A., Husein, M.M., Schaffie, M., Ranjbar, M.: A review on zeolitic imidazolate frameworks use for crude oil spills cleanup. Adv. Geo-Energy Res. **3**(3), 320–342 (2019). https://doi.org/10.26804/ager.2019.03.10
30. Zango, Z.U., Sambudi, N.S., Jumbri, K., Abu Bakar, N.H.H., Abdullah, N.A.F., Negim, E.S.M., Saad, B.: Experimental and molecular docking model studies for the adsorption of polycyclic aromatic hydrocarbons onto UiO-66(Zr) and NH_2-UiO-66(Zr) metal-organic frameworks. Chem. Eng. Sci. p. 115608 (2020). https://doi.org/10.1016/j.ces.2020.115608
31. Jamali, A., Shemirani, F., Morsali, A.: A comparative study of adsorption and removal of organophosphorus insecticides from aqueous solution by Zr-based MOFs. J. Ind. Eng. Chem. **80**, 83–92 (2019). https://doi.org/10.1016/j.jiec.2019.07.034
32. Yang, J.M., Ying, R.J., Han, C.X., Hu, Q.T., Xu, H.M., Li, J.H., Wang, Q., Zhang, W.: Adsorptive removal of organic dyes from aqueous solution by a Zr-based metal-organic framework: effects of Ce(III) doping. Dalt. Trans. **47**(11), 3913–3920 (2018). https://doi.org/10.1039/c8dt00217g
33. Bayazit, S.S., Sąhin, S.: Acid-modulated zirconium based metal organic frameworks for removal of organic micropollutants. J. Environ. Chem. Eng. **8**(5) (2020). https://doi.org/10.1016/j.jece.2020.103901
34. Alamgir, Talha, K., Wang, B., Liu, J.H., Ullah, R., Feng, F., Yu, J., Chen, S., Li, J.R.: Effective adsorption of metronidazole antibiotic from water with a stable Zr(IV)-MOFs: Insights from DFT, kinetics and thermodynamics studies. J. Environ. Chem. Eng. **8**(1), p. 103642 (2020). https://doi.org/10.1016/j.jece.2019.103642
35. Shi, M., Huang, R., Qi, W., Su, R., He, Z.: Synthesis of superhydrophobic and high stable Zr-MOFs for oil-water separation. Colloids Surfaces A Physicochem. Eng. Asp. **602**, p. 125102 (2020). https://doi.org/10.1016/j.colsurfa.2020.125102
36. Yan, F., Liu, Z.Y., Chen, J.L., Sun, X.Y., Li, X.J., Su, M.X., Li, B., Di, B.: Nanoscale zeolitic imidazolate framework-8 as a selective adsorbent for theophylline over caffeine and diprophylline. RSC Adv. **4**, 33047–33054 (2014). https://doi.org/10.1039/c4ra05293e
37. Zango, Z.U., Ramli, A., Jumbri, K., Soraya, N., Ahmad, H.I., Hana, N., Abu, H., Saad, B.: Optimization studies and artificial neural network modeling for pyrene adsorption onto UiO-66(Zr) and NH_2-UiO-66(Zr) metal organic frameworks. Polyhedron **192**, p. 114857 (2020). https://doi.org/10.1016/j.poly.2020.114857
38. Zhang, W., Yang, J.M., Yang, R.N., Yang, B.C., Quan, S., Jiang, X.: Effect of free carboxylic acid groups in UiO-66 analogues on the adsorption of dyes from water: plausible mechanisms for adsorption and gate-opening behavior. J. Mol. Liq. **283**, 160–166 (2019). https://doi.org/10.1016/j.molliq.2019.03.100
39. Sun, W., Li, H., Li, H., Li, S., Cao, X.: Adsorption mechanisms of ibuprofen and naproxen to UiO-66 and UiO-66-NH_2: batch experiment and DFT calculation. Chem. Eng. J. **360**, 645–653 (2019). https://doi.org/10.1016/j.cej.2018.12.021
40. Noor, T., Raffi, U., Iqbal, N., Yaqoob, L., Zaman, N.: Kinetic evaluation and comparative study of cationic and anionic dyes adsorption on Zeolitic Imidazolate frameworks based metal organic frameworks. Mater. Res. Express. **6**(12) (2019)
41. Sun, S., Yang, Z., Cao, J., Wang, Y., Xiong, W.: Copper-doped ZIF-8 with high adsorption performance for removal of tetracycline from aqueous solution. J. Solid State Chem. **285,** p. 121219 (2020). https://doi.org/10.1016/j.jssc.2020.121219

Cek Turnitin - Jurnal - UiO-66 and ZIF-8 Metal-organic Frameworks for Acenaphthene Adsorption

ORIGINALITY REPORT

22%	13%	21%	4%
SIMILARITY INDEX	INTERNET SOURCES	PUBLICATIONS	STUDENT PAPERS

MATCH ALL SOURCES (ONLY SELECTED SOURCE PRINTED)

8%

★ Zakariyya Uba Zango, Anita Ramli, Khairulazhar Jumbri, Nonni Soraya Sambudi et al. "Optimization studies and artificial neural network modeling for pyrene adsorption onto UiO-66(Zr) and NH2-UiO-66(Zr) metal organic frameworks", Polyhedron, 2020

Publication

Exclude quotes	On	Exclude matches	< 1%
Exclude bibliography	On		